Theoretical Mechanism Study of UF_6 Hydrolysis in the Gas Phase

Shao-Wen Hu,* Xiang-Yun Wang, Tai-Wei Chu, and Xin-Qi Liu

Department of Applied Chemistry, College of Chemistry and Molecular Engineering, Peking University, Beijing, China 100871

Received: May 28, 2008; Revised Manuscript Received: June 30, 2008

The mechanism of the gas-phase reaction $UF_6 + H_2O \rightarrow UOF_4 + 2HF$ is explored using relativistic density functional theory calculations. Initially, H_2O coordinates with UF_6 to form a 1:1 complex $UF_6 \cdot H_2O$. Over an activation energy barrier of about 19 kcal/mol, H_2O transfers a H atom to a nearby ligand F, resulting in $UF_5OH + HF$. The eliminated HF or another H_2O molecule may form a hydrogen bond with UF_5OH. Starting from UF_5OH, the second HF elimination results in UOF_4. If UF_5OH is in the isolated form, $UF_5OH \rightarrow UOF_4 + HF$ takes place over a barrier of 24 kcal/mol. If UF_5OH is hydrogen-bonded with H_2O or HF, the conversion barrier is less than 10 kcal/mol. Once formed, the unstable UOF_4 tends to associate with additional ligands and hydrogen-bonding donors. The calculated binding energies indicate the significance of such interactions, which may have profound impact on further HF eliminating reactions. The IR spectra features can be used to indicate the formation and interaction type of the intermediates and products.

I. Introduction

In the nuclear fuel reprocessing industry, hydrolysis of uranium hexafluoride (UF_6) in the gas phase is applied to produce pure nuclear fuel, uranium dioxide (UO_2).[1,2]

$$UF_6 + 2H_2O \rightarrow UO_2F_2 + 4HF$$

$$UO_2F_2 + H_2 \rightarrow UO_2 + 2HF$$

It was found that the initial ratio of UF_6 and H_2O is determinant to the particle size and structure of the intermediate solid product, uranyl fluoride (UO_2F_2), which then influences the property of the final product, UO_2.[3−6] Because UF_6 is a volatile radioactive compound, it can release into the atmosphere and probably reacts with vapor water. The consequent hazard results have been drawing environmental concern.[7−11] To understand the mechanism of UF_6 hydrolysis in the gas phase is clearly of fundamental importance in practice as well as in the theory of actinide chemistry. In contrast to the necessity, kinetic data on this reaction are rare in literature. In an earlier work, Kessie[12] deduced a rate equation of the gas-phase UF_6 hydrolysis based on rate measurements on a packed bed at room temperature, suggesting that the overall reaction was complicated involving both gas and solid phases. It is generally agreed that the hydrolysis reaction includes two major steps.[13]

$$UF_6 + H_2O \rightarrow UOF_4 + 2HF \quad \text{(I)}$$

$$UOF_4 + H_2O \rightarrow UO_2F_2 + 2HF \quad \text{(II)}$$

Klimov et al.[14] measured the rate of the reaction via monitoring concentration of HF and concluded that the first step was rate-limiting. Sherrow and Hunt[15] performed inert gas matrix isolation of the UF_6/H_2O system and measured FTIR spectra during photolysis. They proposed that a 1:1 complex formed prior to production of UOF_4. It is clear, however, that more details are required to reveal the mechanism. Theoretical studies are now widely used to provide indispensable information on reaction mechanism for many molecular systems. For compounds containing actinides, the relativistic effect, electron correlation, and spin−orbit interaction are significant. To include these effects is more computationally demanding. So far, various approximation methods have been applied to molecular and ionic systems containing uranium.[16−26] In a very recent work, Shamov et al.[16] performed a comparative relativistic density functional theory (DFT) and ab initio study on the structures and thermodynamic properties of all probable uranium oxofluorides. They concluded that hybrid density functional shows good agreement in bond dissociation energies with available experimental data. The same conclusion was also made by Batista et al.[20] in an earlier study on bond dissociation energies of UF_6 to UF_5 and Peralta et al.[23] in a hybrid density functional study on UF_n and UCl_n ($n = 1-6$). The density functional with general gradient approximation (GGA), however, is much less time-consuming in computation. It can give better vibration frequencies for systems containing a U=O bond.[16] In this work, therefore, we choose the two DFT methods to explore the potential energy surfaces (PES) of the UF_6/H_2O system. The purpose is to reveal initial reaction channels of UF_6 hydrolysis.

II. Calculation Method

For geometry optimization, we selected the GGA density functional. The parametrization of electron gas data given by Vosko, Wilk, and Nusair[27] (VWN) was used as the local density approximation (LDA) part. The proposals of Becke and Perdew−Wang[28−30] were used as the nonlocal gradient correction. Because uranium involved in the reaction $UF_6 + H_2O \rightarrow UOF_4 + 2HF$ has a closed valance shell electronic structure $5f^06d^07s^0$, the spin−orbit coupling effect should be small in this work. All the calculations were spin-restricted. Relativistic effect was evaluated using scalar zero-order regular approximation (ZORA).[31−33] The geometry structures of all stationary points were fully optimized using the GGA method incorporated with the all-electron ZORA relativistic triple-ζ basis set plus two polarization functions (TZ2P) until the maximum component of the energy gradient became less than 10^{-4} au. For all the stationary points located on the PES, analytical frequency calculations using the same GGA method were performed to characterize their nature as well as to provide zero-point

* Corresponding author. E-mail: swhu@pku.edu.cn.

10.1021/jp804797a CCC: $40.75
Published on Web 08/23/2008

TABLE 1: Bond Lengths of UF_6 and UOF_4 and Vibration Frequencies of UF_6

	R (Å)	freq (cm^{-1})					
UF_6	R_{U-F}	T_{2u}	T_{1u}	T_{2g}	E_g	T_{1u}	A_{1g}
calcd[a]	2.021	133	174	186	515	595	625
scaled[b]		141	185	198	547	632	664
exptl[c]	1.996	143	186	200	534	626	667
	C_{3v}			C_s			
UOF_4	R_{U-O}	R_{U-F}	R_{U-F}	R_{U-O}	R_{U-F}	R_{U-F}	R_{U-F}
PBE(0)[d]	1.761	1.971	2.043	1.810	2.014	2.052	2.047
MP2[d]	1.809	1.993	2.053				
GGA[a]	1.801	1.999	2.064	1.804	2.011	2.055	2.049

[a] DFT GGA calculated results in this work. [b] The GGA calculated frequencies scaled by a factor, 1.063. [c] Experimental data of bond length from ref 39, frequencies from ref 40. [d] Calculated results from ref 16. See Figure 2 for bond lengths specification.

TABLE 2: Relative Energies and Dipole Moments of the Species

species	sym[a]	ΔE_G[b]	ΔE_Z[c]	ΔE_H[d]	$\Delta E_H + \Delta E_Z$	dipole[e]
UF_6OH_2						
$UF_6 \cdot H_2O$ (**1**)	$C_s(0)$	0.00	0.00	0.00	0.00	3.245
$UF_5OH \cdot HF$ (**4**)	$C_s(0)$	5.53	−0.82	4.89	4.07	1.000
$UF_5OH \cdot HF$ (**2**)	$C_s(0)$	8.73	−1.21	8.87	7.66	2.816
$UOF_4 \cdot 2HF$ (**5**)	$C_s(0)$	13.64	−0.93	11.81	10.88	2.184
TS3	$C_s(1)$	14.63	−3.27	15.57	12.30	1.436
TS1	$C_1(1)$	17.67	−1.97	20.79	18.82	2.714
$UF_5O_2H_3$						
$UF_5OH \cdot H_2O$ (**6**)	$C_1(0)$	0.00	0.00	0.00	0.00	4.513
$UOF_4 \cdot HF \cdot H_2O$ (**7**)	$C_1(0)$	5.68	−0.05	3.21	3.16	5.810
TS4	$C_1(0)$	6.08	−0.58	5.44	4.85	5.954
UF_5OH						
UF_5OH	$C_s(0)$	0.00	0.00	0.00	0.00	2.454
UOF_4HF (**3**)	$C_s(0)$	17.84	−0.05	13.08	13.03	4.342
TS2	$C_s(1)$	24.32	−1.63	25.51	23.89	0.884
UF_4O						
UOF_4 (II)	$C_{3v}(0)$	0.00	0.00	0.00	0.00	0.327
UOF_4 (I)	$C_s(0)$	0.06	0.02	1.68	1.70	2.670

[a] Point group of the species; number of imaginary frequency is in parentheses. [b] Relative energy (kcal/mol) of the GGA calculation. [c] Relative ZPE (kcal/mol) of the GGA calculation. [d] Relative energy (kcal/mol) of the hybrid PBE0 calculation. [e] Dipole moments are in debye, hybrid PBE0 calculation.

vibration energy (ZPE) and infrared (IR) spectra data. Intrinsic reaction coordinate (IRC) calculations were performed for each transition state to ensure the correct connections between relevant reactant and product. Using each GGA optimized structure, a single-point calculation using the hybrid density functional (25% Hartree−Fock exchange) PBE0[34−36] incorporated with the all-electron TZ2P basis set and scalar relativistic ZORA was performed. The final energies reported were at the hybrid PBE0 level with GGA calculated ZPE corrections. The relative energies calculated using the two methods are listed comparatively in Table 2.

The interaction energy of molecular fragments in complexes was evaluated. For reaction A + B → AB, the structures of the three molecules A, B, and AB were fully optimized separately. The energy difference, $E_{AB} - E_A - E_B$, was then calculated and corrected by basis set superposition error (BSSE) and ZPE. This was referred to as binding energy (E_{bi}, Table 3). For all the energy items, the hybrid density functional PBE0 calculated results were used except for ZPE, for which the GGA calculated results were used.

Mayer bond orders[37] were calculated using the hybrid PBE0 method for all the stationary points on the PES. In Table 4, we listed the bond orders of U−O and the weakest U−F bonds for all the species.

TABLE 3: Binding Energies of Molecular Fragments in Complexes

associations	ΔE[a]	ΔE[b]	BSSE[b]	ΔE_z[a]	E_{bi}[c]
$UF_6 + H_2O \rightarrow$					
$UF_6 \cdot H_2O$ (**1**)	−1.70	−2.64	−0.74	1.76	−0.14
$UF_5OH + HF \rightarrow$					
$UF_5OH \cdot HF$ (**2**)	−3.49	−3.57	−0.60	1.87	−1.10
$UF_5OH \cdot HF$ (**4**)	−6.69	−7.55	−0.67	2.25	−4.63
$UF_5OH + H_2O \rightarrow$					
$UF_5OH \cdot H_2O$ (**6**)	−10.38	−10.99	−0.54	2.34	−8.11
$UOF_4 + HF \rightarrow$					
$UOF_4 \cdot HF$ (**3**)	−10.16	−10.99	−0.67	1.31	−9.00
$UOF_4 \cdot HF$ (**3**) + HF →					
$UOF_4 \cdot 2HF$ (**5**)	−16.42	−13.71	−0.89	2.19	−10.63
$UOF_4 \cdot HF$ (**3**) + H_2O →					
$UOF_4 \cdot HF \cdot H_2O$ (**7**)	−22.54	−20.85	−0.82	2.33	−17.70

[a] Energies (kcal/mol) of GGA calculations. [b] Energies (kcal/mol) of hybrid PBE0 calculations. [c] Binding energies of the hybrid PBE0 calculation. See section II for definition.

TABLE 4: Mayer Bond Order of the Species[a]

species	U−F[b]	U−O
UF_6	0.867	
UOF_4 (I)	0.696	2.091
UOF_4 (II)	0.696	2.091
$UF_6 \cdot H_2O$ (**1**)	0.811	0.136
TS1	0.267	0.571
$UF_5OH \cdot HF$ (**2**)	0.011	0.903
UF_5OH	0.759	0.901
TS2	0.290	1.394
$UOF_4 \cdot HF$ (**3**)	0.085	2.040
$UF_5OH \cdot HF$ (**4**)	0.670	0.998
TS3	0.248	1.463
$UOF_4 \cdot 2HF$ (**5**)	0.150	1.749
$UF_5OH \cdot H_2O$ (**6**)	0.740	1.203
TS4	0.371	1.630
$UOF_4 \cdot HF \cdot H_2O$ (**7**)	0.216	1.845

[a] Results of the hybrid PBE0 calculation. [b] The weakest U−F bond of the species.

The ADF2006 program package[38] was employed. The accuracy criterion of 6.5 was used for all the numerical integrations, which is a rough indication of the number of significant digits.

III. Results and Discussion

This section consists of five parts. In part III.1, we discuss briefly the accuracy of the results obtained in this work. In part III.2, we show the geometries and the energies of a probable interaction between UF_6 and H_2O and formation of UF_5OH after first HF elimination. In part III.3, we show the geometries and the energies of conversion between UF_5OH and UOF_4 + HF or second HF elimination. In part III.4, total reaction pathways are overviewed. In part III.5, we show the calculated IR spectra features of the species and compare with experimental data.

Each minimum structure of the complexes on the PES is named according to its structure and numbered as it appears in the discussion. The symbol "TS" plus a number is used to name each transition state.

III.1. About the Accuracy of the Results Obtained in This Work. The structure and vibration frequencies of isolated UF_6 have been studied experimentally[39,40] as well as theoretically (see refs 20−26 and references therein). In Table 1, we list the geometry parameter and vibration frequencies of UF_6 calculated

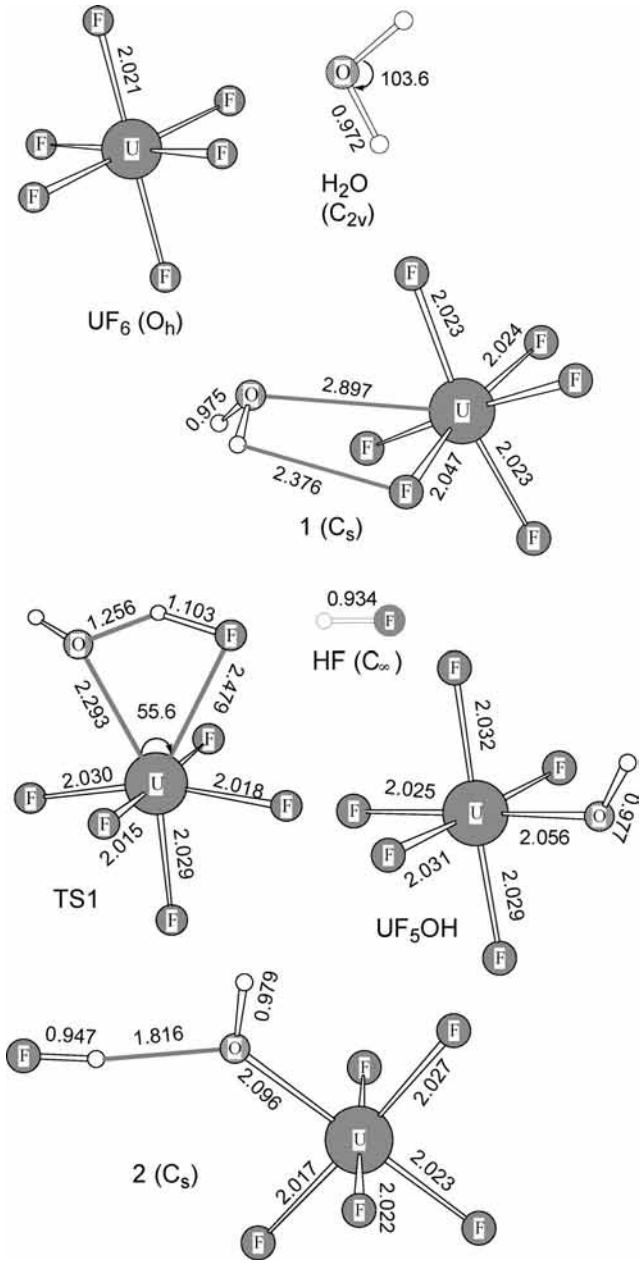

Figure 1. Species involved in formation of $UF_6 \cdot H_2O$, UF_5OH, and $UF_5OH \cdot HF$; bond lengths are in angstroms; angles are in deg; in parentheses, the symmetry of the species is indicated except for C_1.

using the GGA DFT method comparatively with experimental data. It can be seen that the GGA calculated results overestimate the U−F bond length slightly and give systematically lower vibration frequencies for UF_6. However, the GGA method can give better vibration frequency for systems containing a U═O bond (see ref 16 and part III.5 of this section) and is computationally efficient for larger molecular systems. Therefore, it is still a reasonable choice to employ the GGA method in this work for all the geometry and frequency calculations.

Kavocs and Konings[19] performed a detailed theoretical study of isolated UOF_4. Shamov et al.[16] also studied the species using different methods. They showed that the two minima conformers of UOF_4 with C_s and C_{3v} symmetry were very close in energy. Although the geometry parameters of UOF_4 varied slightly using different methods (Table 1), it seems hard to tell which methods gave a better structure data due to lack of relevant experimental results. We labeled the two conformers as UOF_4 (I) and UOF_4 (II) (Figure 2). Consistent with the former studies, the energies of UOF_4 (I) and UOF_4 (II) are almost same in both GGA and PBE0 calculations performed in this work. The C_s conformer UOF_4 (I) has a much larger dipole moment, and its ZPE is slightly larger (Table 2). The calculated vibration frequency of the U═O bond using the GGA method is in good agreement with experimental data (see part III.5, Table 5).

The essential part of UF_6 hydrolysis involves breaking of the U−F bond and formation of the U−O and U═O bonds. Therefore, the computation model employed should be able to evaluate bond dissociation energies accurately. Our choice of the method is based largely upon previous theoretical works. In particular, Shamov et al.[16] gave a thorough investigation on the performance of various DFT methods when applied to uranium oxofluorides. In comparison with experimental data as well as two wave function based theoretical methods, MP2 and CCSD(T), they concluded that the hybrid DFT method PBE0 can describe bond dissociation energies better than MP2 and close to the CCSD(T) method. Therefore, we choose the hybrid PBE0 method to calculate the energies and other electronic properties in this work. Because it is interesting to see the performance of the less expensive GGA method in energy evaluation, the relative energies and binding energies of the species calculated using the GGA and the hybrid PBE0 methods are listed comparatively in Tables 2 and 3. It can be seen that the largest discrepancy between energies calculated using the two DFT methods is less than 5 kcal/mol. For binding energy of fragments in complexes, the BSSE is relatively small. The major part of the correction comes from the ZPE.

Weak molecular interactions are known to be not well described with DFT methods. In this work, two or three species $UF_6 \cdot H_2O$ (**1**) and $UF_5OH \cdot HF$ may be regarded as complexes formed via such weak interactions (binding energies of molecular fragments in the complexes are less than 5 kcal/mol). Their geometries and binding energies might vary if theoretical methods used were more accurate on this aspect. In this work, however, these kinds of interactions are relative small and do not influence the major conclusion. Other theoretical methods are thus not employed.

III.2. Formation of $UF_6 \cdot H_2O$ and $UF_5OH \cdot HF$. At the initial stage before reaction, the two molecules UF_6 and H_2O can form the complex $UF_6 \cdot H_2O$ (**1**) (Figure 1), in which H_2O coordinates to uranium as an outer-sphere ligand. The distance between uranium and oxygen is 2.898 Å, considerable longer than the bond length of U−F (2.023 Å), indicating the U−O association is weak. As H_2O approaches, the symmetry of UF_6 changes from O_h to C_s. The three U−F bonds on the side of the incoming H_2O bend away slightly. For the two F ligands close to the two H of H_2O, the U−F bonds become slightly longer, indicating a weak attraction between H and F. Consistent with the weak interaction, the binding energy of UF_6 and H_2O in **1** is −0.14 kcal/mol (Table 3). The calculated dipole moment (Table 2) of **1** is larger than that of H_2O, indicating a Lewis acid−base interaction or electron-transfer effect. Several other initial nuclear positions have been tested. Frequency calculations showed that the other stationary structures were not minima on the PES and their energies were relatively higher. Consequently, the molecular interaction between UF_6 and H_2O is mainly in coordinated form **1**. Sherrow and Hunt[15] observed new IR absorption spectra after gases UF_6 and H_2O were codeposited in Ar matrix. The intensity of these new absorptions appeared to be directly related to the UF_6 and H_2O gas-phase interaction prior to the deposition, since annealing the matrix after deposition failed to produce any significant change to the product band. This observation led them to the conclusion that a 1:1

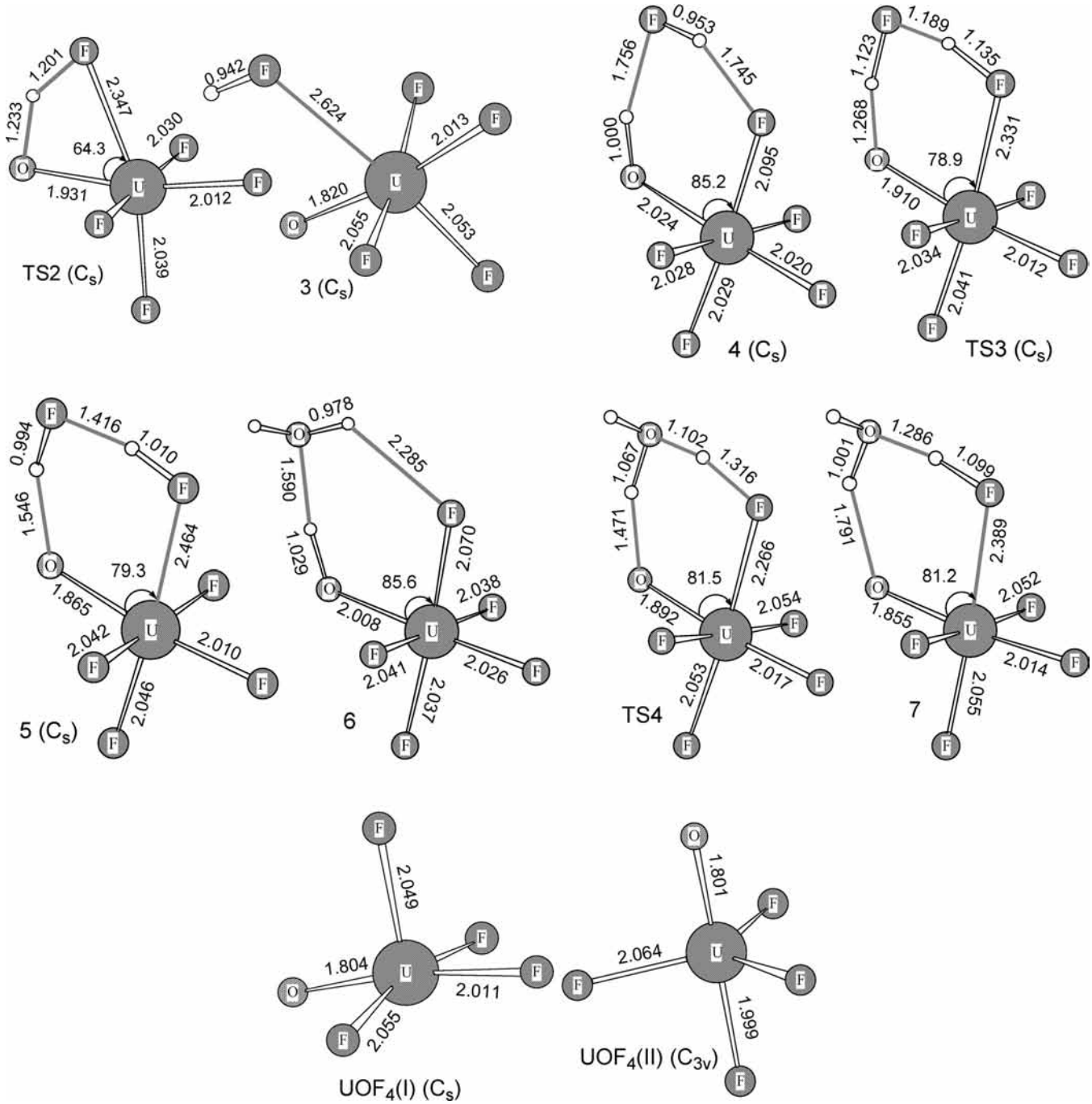

Figure 2. Species involved in formation of $UOF_4 \cdot HF$, $UOF_4 \cdot 2HF$, and $UOF_4 \cdot HF \cdot H_2O$; bond lengths are in angstroms; angles are in deg; in parentheses, the symmetry of each species is indicated except for C_1.

complex $UF_6 \cdot H_2O$ forms in the gas phase. However, the inert gas played a role in their work. In part III.5, we shall compare the calculated frequency spectra with the relevant experimental observation.

The reaction of UF_6 and H_2O starts via transition state TS1, in which H_2O approaches to uranium and transfers one of its hydrogen atoms to a fluorine atom simultaneously. A four-member ring structure with a bridge hydrogen bond, O−H−F, appears in TS1. The ring is almost in the same plane with the other three fluorine ligands. Frequency and IRC calculations of TS1 show that TS1 is a transition state connecting reactant **1** to a product, complex $UF_5OH \cdot HF$ (**2**), in which the eliminated HF is hydrogen-bonded with molecule UF_5OH. Relative to **1**, the energies of TS1 and **2** are 18.82 and 7.66 kcal/mol, indicating that $UF_6 \cdot H_2O$ (**1**) → $UF_5OH \cdot HF$ (**2**) is an endothermic reaction with a certain activation energy. Besides geometry, the electronic structure changes can be seen from Mayer bond orders of the relevant bonds (Table 4). From **1** to TS1 to **2**, the order of U−O increases from 0.136 to 0.571 to 0.903, whereas the order of one U−F bond decreases from 0.811 to 0.267 to 0.011.

To our knowledge, there is no experimental or theoretical information about the intermediate molecule UF_5OH. According to our work, however, UF_5OH should be the first product during UF_6 hydrolysis. The minimum structure of UF_5OH has C_s symmetry with a zero dihedral angle H−O−U−F. The U−OH bond is only slightly longer than a U−F bond. The bond order is 0.901, close to the order of a U−F bond. These features show that UF_5OH is structurally close to UF_6. Complex $UO_2(OH)_2$ and anion $[UO_2(OH)_4]^{2-}$ have been studied theoretically in

TABLE 5: Specific Vibration Frequencies of the Species[a]

species	calcd[b] H−O−H	exptl[c]
H_2O	1596(73)	
$UF_6 \cdot H_2O$ (**1**)	1586(77)	1588, 1586
$UF_5OH \cdot H_2O$ (**6**)	1591(68)	
$UOF_4 \cdot HF \cdot H_2O$ (**7**)	1233(94), 1463(644), 1490(633), 1656(1220)	

species	calcd[b] F(O)−H	calcd[b] U═O	exptl[c]
UOF_4 (I)		853(137)	857
UOF_4 (II)		860(135)	868
HF	3951(101)		
H_2O	3758(49)		
$UOF_4 \cdot HF$ (**3**)	3799(152)	833(134)	3718
UF_5OH	3656(244)		
$UF_5OH \cdot HF$ (**2**)	3653(1012), 3630(168)		3625, 3623
$UF_5OH \cdot HF$ (**4**)	3566(657), 3232(744)	862(77)	
$UOF_4 \cdot 2HF$ (**5**)	2928(2222), 2477(470)	752(243)	
$UF_5OH \cdot H_2O$ (**6**)	3711(116), 2724(2543)	866(89)	
$UOF_4 \cdot HF \cdot H_2O$ (**7**)	3674(130), 3219(720)	706(275)	

[a] Frequencies are in cm^{-1}; intensities (in parentheses) are in km/mol. [b] Results of GGA calculations in this work. [c] Measured FTIR data from ref 15.

detail.[17,18,21] We notice that UF_5OH is quite different from $UO_2(OH)_4^{2-}$ and $UO_2(OH)_2$ structurally. The U−OH bond length in the latter complexes is considerable longer than a usual U−F bond due to the existence of fragment O═U═O.

III.3. Formation of $UOF_4 \cdot HF$, $UOF_4 \cdot 2HF$, and $UOF_4 \cdot HF \cdot H_2O$. Upon formation, UF_5OH can eliminate another HF molecule via a bridge hydrogen bond O−H−F (TS2, Figure 2). A hydrogen atom transfers from the OH group to one of the adjacent F atoms. As H transfers, the U−O bond becomes shorter and the U−F(H) bond becomes longer, resulting in complex $UOF_4 \cdot HF$ (**3**), UOF_4 coordinated by the eliminating HF molecule. The calculated U−O bond order in **3** is 2.040 (Table 4), showing clearly that it is a double bond. The U−F(H) bond order in **3** is 0.085. The energies of TS2 and **3** are 23.89 and 13.03 kcal/mol relative to UF_5OH (Table 2), indicating that the conversion, $UF_5OH \rightarrow UOF_4 \cdot HF$, is an endothermic process over a quite high barrier.

Besides existing as a simple molecule, UF_5OH probably associates with HF through a complicated hydrogen bond, F···H−F···H−O, resulting in complex $UF_5OH \cdot HF$ (**4**), in which HF accepts a hydrogen bond from the OH group and donates one to a F ligand. The energy of **4** is 3.59 kcal/mol lower than that of the single hydrogen-bonded complex **2**. The binding energy of HF and UF_5OH in **4** is −4.63 kcal/mol, 3.53 kcal/mol stronger than that of **2**, accounting for the reason of stabilization. Starting from complex **4**, H transfers from the OH group to the F atom with HF as a media. The transition state is TS3. Along with H transfer, the U−OH bond shortens and the U−F(H) bond lengthens. The product is $UOF_4 \cdot 2HF$ (**5**), UOF_4 coordinated by HF and hydrogen-bonded with another HF molecule. From **4** to TS3 to **5**, the bond order of the U−O bond increases from 0.998 to 1.463 to 1.749 while the bond order of U−F(H) bond decreases from 0.670 to 0.248 to 0.150. It can be seen that the hydrogen bonding influences the U−O bond order slightly. In complex **4**, the U−O bond order is slightly larger than a usual single bond, whereas in **5**, the U−O bond order is slightly smaller than a usual double bond.

Besides HF, a surrounding H_2O molecule can also form a complex with UF_5OH. In this complex $UF_5OH \cdot H_2O$ (**6**), H_2O acts both as a H donor and an acceptor. The binding energy is −8.11 kcal/mol, 3.48 kcal/mol larger than that of **4**. Therefore, H_2O can form a more stable complex with UF_5OH. Geometrically, H_2O is closer to the U−OH group in **6**.

Starting from complex **6**, similarly, H transfers with H_2O as a media. The transition state is TS4. The product is $UOF_4 \cdot HF \cdot H_2O$ (**7**), UOF_4 coordinated by HF and hydrogen-bonded with a H_2O molecule. From **6** to TS4 to **7**, the bond order of the U−O bond changes from 1.203 to 1.630 to 1.845 while the bond order of the U−F(H) bond decreases from 0.740 to 0.371 to 0.216. In complex **6**, the U−O bond order is clearly larger than 1, indicating some double-bonding character.

The energy barriers of the two processes are 8.23 and 4.85 kcal/mol, respectively. Therefore, the conversion from UF_5OH to UOF_4 + HF appears much easier with the help of HF or H_2O. In comparison with HF, H_2O is more effective as a hydrogen shuttle. Hratchian et al.[17] studied the H_2O-catalyzed conformational change of $UO_2(OH)_2$. They concluded that in the gas phase, the energy barrier was about 20 kcal/mol lower with the help of H_2O. A similar effect occurs in our systems.

The energies of **5** and **7** are 6.81 and 3.16 kcal/mol higher than those of **4** and **6**. Although the conversion from UF_5OH to UOF_4 + HF in these associated species is endothermic, the energy differences between reactant and product are a few kcal/mol smaller than that of the isolated ones. However, it should be mentioned that the U−O bond orders in **5** and **7** are 1.749 and 1.845, respectively, smaller than that of a U−O double bond (2.040) in **3**.

III.4. Overview of the Reaction Channels. The pathways of the reaction $UF_6 + H_2O \rightarrow UOF_4 + 2HF$ are drawn schematically in Figure 3. On the basis of the theoretical evidence provided in this work, the total reaction probably includes following elementary steps:

In the initial stage, H_2O associates with UF_6 to form a weak 1:1 complex.

$$UF_6 + H_2O \rightarrow UF_6 \cdot H_2O\ (\mathbf{1})$$

$$\Delta E = -0.14\ \text{kcal/mol} \quad (1)$$

Over an energy barrier, the first HF eliminates and hydrogen bonds to UF_5OH. According to the height of the barrier, this step is rate-limiting.

$$UF_6 \cdot H_2O\ (\mathbf{1}) \rightarrow UF_5OH \cdot HF\ (\mathbf{2})$$

$$E_a = 18.82\ \text{kcal/mol}$$

$$\Delta E = 7.66\ \text{kcal/mol} \quad (2)$$

The hydrogen bond in **2** is easy to break.

$$UF_5OH \cdot HF\ (\mathbf{2}) \rightarrow UF_5OH + HF$$

$$\Delta E = 1.10\ \text{kcal/mol} \quad (3)$$

For isolated UF_5OH, the second HF elimination is another rate-limiting step. The product is a complex of UOF_4 coordinated by HF.

$$UF_5OH \rightarrow UOF_4 \cdot HF\ (\mathbf{3})$$

$$\Delta E_a = 23.89\ \text{kcal/mol}$$

$$\Delta E = 13.03\ \text{kcal/mol} \quad (4)$$

Otherwise, UF_5OH may associate with a surrounding HF or H_2O molecule.

$$UF_5OH + HF \rightarrow UF_5OH \cdot HF\ (\mathbf{4})$$

$$\Delta E = -4.63\ \text{kcal/mol} \quad (5)$$

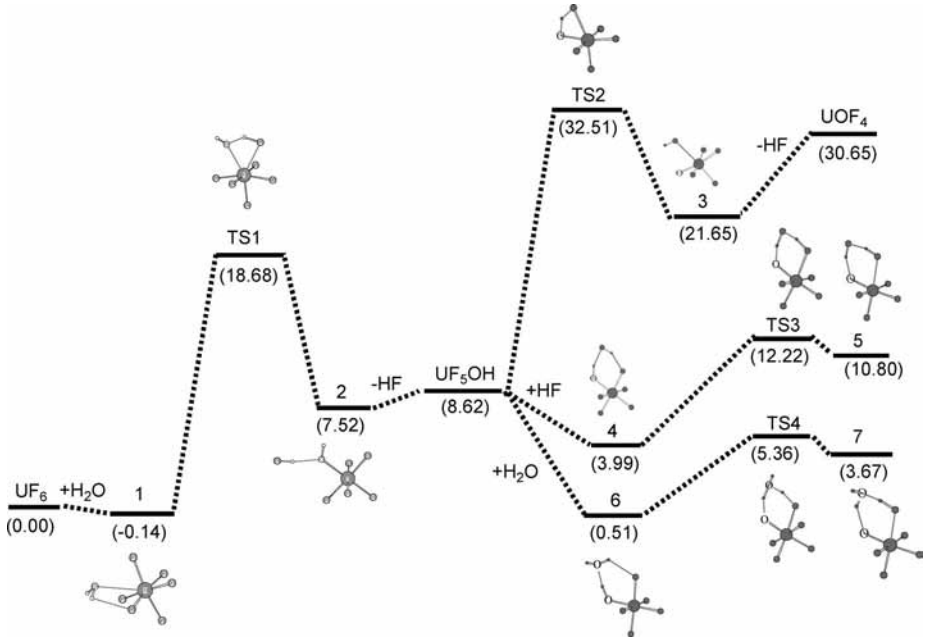

Figure 3. Pathways of reaction $UF_6 + H_2O \rightarrow UOF_4 + 2HF$; the relative energies (in parentheses) are in kcal/mol.

$$UF_5OH + H_2O \rightarrow UF_5OH \cdot H_2O\ (\mathbf{6})$$

$$\Delta E = -8.11\ \text{kcal/mol} \quad (6)$$

It can be seen that both associations stabilize UF_5OH. H_2O has more stabilization effect than HF. In these associated forms, the second HF elimination can be realized through HF or H_2O-helped H transfer. The energy barriers are considerably lowered due to the catalysis. H_2O is a more effective catalyst than HF.

$$UF_5OH \cdot HF\ (\mathbf{4}) \rightarrow UOF_4 \cdot 2HF\ (\mathbf{5})$$

$$\Delta E_a = 8.23\ \text{kcal/mol}$$

$$\Delta E = 6.81\ \text{kcal/mol} \quad (7)$$

$$UF_5OH \cdot H_2O\ (\mathbf{6}) \rightarrow UOF_4 \cdot HF \cdot H_2O\ (\mathbf{7})$$

$$E_a = 4.85\ \text{kcal/mol}$$

$$\Delta E = 3.16\ \text{kcal/mol} \quad (8)$$

As an intermediate product of UF_6 hydrolysis, UOF_4 tends to be coordinated by HF and hydrogen-bonded by another HF or H_2O. According to the calculated binding energies, dissociation of the complex **7** is energy demanding. In other words, the species **3** and **5** may convert to the more stable one, **7**.

$$UOF_4 \cdot HF\ (\mathbf{3}) \rightarrow UOF_4 + HF$$

$$\Delta E = 9.00\ \text{kcal/mol} \quad (9)$$

$$UOF_4 \cdot 2HF\ (\mathbf{5}) \rightarrow UOF_4 \cdot HF\ (\mathbf{3}) + HF$$

$$\Delta E = 10.63\ \text{kcal/mol} \quad (10)$$

$$UOF_4 \cdot HF \cdot H_2O\ (\mathbf{7}) \rightarrow UOF_4 \cdot HF\ (\mathbf{3}) + H_2O$$

$$\Delta E = 17.70\ \text{kcal/mol} \quad (11)$$

We can see from Figure 3 that the initial steps of UF_6 hydrolysis in the gas phase are endothermic and require substantial activation energy. Appropriate association of UOF_4 with surrounding molecules can stabilize the reaction system. Upon formation, the molecular fragments bond together strongly as complex $UOF_4 \cdot HF \cdot H_2O$.

III.5. Vibration Frequency Spectra of the Species. IR spectra measurement is a useful tool in studying gas-phase reactions. For the reaction of UF_6 and H_2O, several absorption bands can signal the formation of intermediate products (Table 5). Among these absorption features, two bands are specific. One can be used to indicate H_2O involvement in coordination; the other can be used to indicate the formation of a U=O bond.

When H_2O coordinates to uranium as a Lewis base, its typical absorption band of H−O−H vibration at 1596 cm^{-1} red-shifts. In complex $UF_6 \cdot H_2O$ (**1**), the band becomes 1586 cm^{-1}. The same absorptions at 1588 and 1586 cm^{-1} were detected by Sherrow and Hunt.[15] On the basis of this observation, they proposed that a 1:1 $UF_6 \cdot H_2O$ complex forms through $U-OH_2$ Lewis acid−base interaction. In this work, we found two other complexes also involved H_2O association. In complex $UF_5OH \cdot H_2O$ (**6**), H_2O does not coordinate with U but acts mainly as a hydrogen-bonding acceptor and donor. The red-shift of the H−O−H vibration is not significant. In complex $UOF_4 \cdot HF \cdot H_2O$ (**7**), H_2O also acts as a hydrogen-bonding acceptor and donor, but the association is stronger. As a result, the vibration band splits into several bands.

Another important spectra feature is the U=O bond vibration absorption. Sherrow and Hunt[15] detected two bands at 857 and 868 cm^{-1} and use them to indicate the formation of UOF_4. According to our calculations, two absorption bands at 853 and 860 cm^{-1} come from isolated UOF_4 (I) and UOF_4 (II). However, UOF_4 is likely to associate with surrounding molecules; the two bands may vary depending on their environment. In particular, when the oxygen of U=O is involved in hydrogen bonding with H_2O or HF, as in complexes $UOF_4 \cdot 2HF$ (**5**) and $UOF_4 \cdot HF \cdot H_2O$ (**7**), the bands red-shift to 752 and 706 cm^{-1}, respectively.

The formation of the U−OH single bond is difficult to detect. For H_2O, the O−H vibration band appears at 3758 cm^{-1}. In the molecule UF_5OH and the complex $UF_5OH \cdot HF$, the calculated O−H vibration band intensifies and red-shifts to 3656 and 3630 cm^{-1}, respectively. Sherrow and Hunt[15] also detected absorption bands at 3718, 3625, and 3623 cm^{-1}. In the presence of HF, however, the absorption of the F−H vibration appears at the same spectra region. The lack of specific IR spectra features may be one reason to explain why UF_5OH remains unknown. For the complexes $UF_5OH \cdot HF$ (**4**) and $UF_5OH \cdot H_2O$ (**6**), the band red-shifts significantly due to involvement of the OH group in hydrogen bonding. Furthermore, because the U−O

bond has some double-bond character in the two species, the absorptions at 862 and 866 cm^{-1} appear, although they are weaker and in a slightly higher frequency region compared with the U═O bond of $UOF_4 \cdot 2HF$ (**5**) and $UOF_4 \cdot HF \cdot H_2O$ (**7**).

IV. Conclusions

In the gas phase, UF_6 and H_2O associate via a weak F_6U-OH_2 Lewis acid−base interaction. Starting from the $UF_6 \cdot H_2O$ complex, the hydrolysis reaction takes place over a barrier of about 19 kcal/mol. The first intermediate product is UF_5OH. The bond length and bond order are similar for U−OH and U−F bonds. The eliminated HF or a H_2O molecule can associate with UF_5OH through hydrogen bonding. Further reaction can proceed via three different channels. In isolated form, UF_5OH converts to $UOF_4 \cdot HF$ over a barrier of 24 kcal/mol. The relatively unstable UOF_4 and $UOF_4 \cdot HF$ tend to associate with additional HF or H_2O through hydrogen bonding or coordination. In associated forms, $UF_5OH \cdot HF$ or $UF_5OH \cdot H_2O$ can convert to $UOF_4 \cdot 2HF$ and $UOF_4 \cdot HF \cdot H_2O$ much easier. However, the products are also highly associated, which may influence further reactions. The calculated IR frequency absorptions are in good agreement with available experimental observation. Two kinds of spectra features are specific to indicate H_2O coordination and formation of a U═O bond. Because the initial steps of UF_6 hydrolysis in the gas phase are endothermic, elevated temperature should be a necessary condition.

Acknowledgment. The authors thank the Computer Center of Peking University for providing the IBM RS/6000 SP3 computer to accomplish the calculations.

References and Notes

(1) Semeraz, J. T.; Carter, R. Eur. Patent No. EP 0712 379 B, 1994.
(2) Schmets, J. J. *At. Energy Rev.* **1970**, *8*, 3.
(3) Hou, R. Z.; Mahmud, T.; Prodromidis, N.; Roberts, K. J.; Williams, R. A.; Goddard, D. T. *Ind. Eng. Chem. Res.* **2007**, *46*, 2020.
(4) Babenko, S. P.; Bad'in, A. V. *At. Energy* **2005**, *99*, 787.
(5) Sazhin, S. S.; Jeapes, A. P. *J. Nucl. Mater.* **1999**, *275*, 231.
(6) Zachariasen, W. H. *Acta Crystallogr., Sect. A* **1948**, *1*, 277.
(7) Brand, R. A.; Schnug, E. *Landbauforsch. Voelkenrode* **2005**, *55*, 211.
(8) Hartmann, H. M.; Monette, F. A.; Avci, H. I. *Hum. Ecol. Risk Assess.* **2000**, *6*, 851.
(9) Nair, S. K.; Chambers, D. B.; Radonjic, Z.; Park, S. *Atmos. Environ.* **1998**, *32*, 1729.
(10) Hanna, S. R.; Chang, J. C.; Zhang, X. M. J. *Atmos. Environ.* **1997**, *31*, 901.
(11) Armstrong, D. P.; Bostick, W. D.; Fletcher, W. H. *Appl. Spectrosc.* **1991**, *45*, 1008.
(12) Kessie, R. W. *Ind. Eng. Chem. Process Des. Dev.* **1967**, *6*, 105.
(13) Weigel, F. *The Chemistry of the Actinide Elements*, 2nd ed.; Chapman and Hall: New York, 1986; Vol. 1, Chapter 5.
(14) Klimov, V. D.; Kravetz, Y. M.; Besmelnitzin, A. V. *J. Fluorine Chem.* **1992**, *58* (2−3), 262.
(15) Sherrow, S. A.; Hunt, R. D. *J. Phys. Chem.* **1992**, *96*, 1095.
(16) Shamov, G. A.; Schreckenbach, G.; Vo, T. N. *Chem.−Eur. J.* **2007**, *13*, 4932.
(17) Hratchian, H. P.; Sonnenberg, J. L.; Hay, P. J.; Martin, R. L.; Bursten, B. E.; Schlegel, H. B. *J. Phys. Chem. A* **2005**, *109*, 8579.
(18) Schreckenbach, G.; Hay, P. J.; Martin, R. L. *Inorg. Chem.* **1998**, *37*, 4442.
(19) Kovacs, A.; Konings, R. *ChemPhysChem.* **2006**, *7*, 455.
(20) Batista, E. R.; Martin, R. L.; Hay, P. J.; Peralta, J. E.; Scuseria, G. E. *J. Chem. Phys.* **2004**, *121*, 2144.
(21) Privalov, T.; Schimmelpfennig, B.; Wahlgren, U.; Grenthe, I. *J. Phys. Chem. A* **2002**, *106*, 11277.
(22) Gagliardi, L.; Willetts, A.; Skylaris, C. K.; Handy, N. C.; Spence, S.; Ioannou, A. G.; Simple, A. M. *J. Am. Chem. Soc.* **1998**, *120*, 11727.
(23) Peralta, J. E.; Batista, E. R.; Scuseria, G. E.; Martin, R. L. *J. Chem. Theory Comput.* **2005**, *1*, 612.
(24) Garcia-Hernandez, M.; Willnauer, C.; Kruger, S.; Moskaleva, L. V.; Rosch, N. *Inorg. Chem.* **2006**, *45*, 1356.
(25) Han, Y. K.; Hirao, K. *J. Chem. Phys.* **2000**, *113*, 7345.
(26) deJong, W. A.; Nieuwpoort, W. C. *Int. J. Quantum Chem.* **1996**, *58*, 203.
(27) Vosko, S. H.; Wilk, L.; Nusair, M. *Can. J. Phys.* **1980**, *58*, 1200.
(28) Becke, A. D. *Phys. Rev. A* **1988**, *38*, 3098.
(29) Perdew, J. P. *Phys. Rev. B* **1986**, *33*, 8822.
(30) Batista, E. R.; Martin, R. L.; Hay, P. J. *J. Chem. Phys.* **2004**, *121*, 11104.
(31) van Lenthe, E.; Ehlers, A.; Baerends, E. J. *J. Chem. Phys.* **1999**, *110*, 8943.
(32) van Lenthe, E.; Baerends, E. J.; Snijders, J. G. *J. Chem. Phys.* **1993**, *99*, 4597.
(33) van Lenthe, E.; Baerends, E. J.; Snijders, J. G. *J. Chem. Phys.* **1994**, *101*, 9783.
(34) Adamo, C.; Barone, V. *J. Chem. Phys.* **1998**, *108*, 664.
(35) Ernzerhof, M.; Scuseria, G. E. *J. Chem. Phys.* **1999**, *110*, 5029.
(36) Adamo, C.; Barone, V. *J. Chem. Phys.* **1999**, *110*, 6158.
(37) Mayer, I. *Chem. Phys. Lett.* **1983**, *97*, 270.
(38) (a) te Velde, G.; Bickelhaupt, F. M.; van Gisbergen, S. J. A.; Guerra, C. F.; Baerends, E. J.; Snijders, J. G.; Ziegler, T. *J. Comput. Chem.* **2001**, *22*, 931. (b) Guerra, C. F.; Snijders, J. G.; te Velde, G.; Baerends, E. J. *Theor. Chem. Acc.* **1998**, *99*, 391. (c) Baerends, E. J.; Autschbach, J.; Berces, A.; Bickelhaupt, F. M.; Bo, C.; Boerrigter, P. M.; Cavallo, L.; Chong, D. P.; Deng, L.; Dickson, R. M.; Ellis, D. E.; van Faassen, M.; Fan, L.; Fischer, T. H.; Guerra, C. F.; van Gisbergen, S. J. A.; Groeneveld, J. A.; Gritsenko, O. V.; Grüning, M.; Harris, F. E.; van den Hoek, P.; Jacob, C. R.; Jacobsen, H.; Jensen, L.; van Kessel, G.; Kootstra, F.; van Lenthe, E.; McCormack, D. A.; Michalak, A.; Neugebauer, J.; Osinga, V. P.; Patchkovskii, S.; Philipsen, P. H. T.; Post, D.; Pye, C. C.; Ravenek, W.; Ros, P.; Schipper, P. R. T.; Schreckenbach, G.; Snijders, J. G.; Solà, M.; Swart, M.; Swerhone, D.; te Velde, G.; Vernooijs, P.; Versluis, L.; Visscher, L.; Visser, O.; Wang, F.; Wesolowski, T. A.; van Wezenbeek, E.; Wiesenekker, G.; Wolff, S. K.; Woo, T. K.; Yakovlev, A. L.; Ziegler, T. *ADF2006.01*; SCM, Theoretical Chemistry Vrije Universiteit: Amsterdam, The Netherlands, 2006; http://www.scm.com.
(39) Seip, H. M. *Acta Chem. Scand.* **1965**, *20*, 2698.
(40) McDowell, R. S.; Asprey, L. B.; Paine, R. T. *J. Chem. Phys.* **1974**, *61*, 3571.

JP804797A